Electronic Supplementary Information (ESI)

Organic Solvent-Free Synthesis of Calcium Sulfate Hemihydrate at Room Temperature

Selina Reigl[a], Alexander E. S. Van Driessche[b], Timo Ullrich[a], Sebastian Koltzenburg[c], Werner Kunz[a] and Matthias Kellermeier*[d]*

[a]Institute of Physical and Theoretical Chemistry, University of Regensburg, Universitätsstr. 31, D-93040 Regensburg, Germany; E-mail: werner.kunz@ur.de

[b]Instituto Andaluz de Ciencias de la Tierra (IACT), CSIC – University of Granada, E-18100 Armilla, Granada, Spain.

[c]BASF SE, Carl-Bosch-Str. 38, D-67056 Ludwigshafen, Germany

[d]Material Science, BASF SE, Carl-Bosch-Str. 38, D-67056 Ludwigshafen, Germany; E-mail: matthias.kellermeier@basf.com

Experimental Procedures

Used Chemicals: Calcium chloride dihydrate (Carl Roth, ≥99 %), calcium sulfate (Sigma-Aldrich, 99 %), calcium sulfate dihydrate (Sigma-Aldrich, 98 %), calcium sulfate hemihydrate (Sigma-Aldrich, 97 %), sodium sulfate (Carl Roth, ≥99 %), sodium hydroxide solution (Carl Roth, 1 M), sodium hydroxide (VWR, 99.5 %), hydrochloric acid (Sigma-Aldrich, 1 M solution), sodium chloride (Carl Roth, ≥99.5 %), lithium chloride (Carl Roth, ≥99 %), sodium acetate trihydrate (Merck, p.a.), sodium 1-pentane sulfonate (SPS; TCI, >98 %), betaine (TCI, anhydrous, >97 %), poly(vinylpyrrolidone) (PVP; Sigma-Aldrich, M ≈ 55.000 Da), polyoxyethylene(2.5) bis(carboxymethyl) ether (cE2.5c; Sigma-Aldrich, M ≈ 250 Da), and polyoxyethylene(10.5) bis(carboxymethyl) ether (cE10.5c; Sigma-Aldrich, M ≈ 600 Da) were used as received. Polyoxyethylene(5) octylether carboxylic acid (C8E5cH; ≥88.5 %), polyoxyethylene(8) octylether carboxylic acid (C8E8cH; ≥87.5 %) and polyoxyethylene(5) lauryl ether carboxylic acid (C12/14E4.5cH; ≥90 %) were supplied by Kao Chemicals and purified by hot-water extraction as described in detail elsewhere.[S1] All solutions and dilutions were prepared using water with a resistivity of 18 MΩ cm obtained from a Millipore system.

Precipitation Experiments: The experimental procedure to precipitate calcium sulfate and isolate the formed particles was developed in our previous studies[S1,S2] and will therefore only be briefly outlined here. Aqueous solutions of $CaCl_2$ (0.8 M) and Na_2SO_4 (0.8 M) were pre-equilibrated at the desired temperature (25 or 40 °C) for 30 min. While NaCl, LiCl and PVP were added at the same concentration to both solutions prior to mixing, carboxylates and sulfonates (all in neutralised form as sodium salts) were introduced in the respective doubled amount via the Na_2SO_4 solution, in order to prevent any pre-complexation with calcium ions. Equal volumes (5 mL) of two solutions were rapidly mixed to generate systems supersaturated with respect to any of the possible $CaSO_4$ phases (0.4 M). After mixing, precipitation was allowed to proceed for 5 min at the desired temperature without further agitation. The formed solid materials were isolated by filtration through Nylon membranes with a pore size of 0.45 µm and subsequent washing with 2 mL water. After drying for 30 min at 40 °C, the mineral phase

composition was analysed by IR spectroscopy. To ensure reproducibility, each experiment was repeated at least twice and mean values were taken for evaluation.

Characterization of Solid Products: For mineral phase identification and quantification, a 670-IR spectrometer from Varian (Palo Alto, USA) was used to collect IR spectra of the isolated precipitates in attenuated total reflection (ATR) mode at a resolution of 1 cm^{-1}. The data was averaged over 16 scans. By correlating measured peak intensities with the bassanite content through a calibration established in our previous work,[S1,S2] the mass fraction of hemihydrate in the precipitates could be determined. Powder X-ray diffraction (PXRD) patterns were acquired for selected samples using a D8 Advance Series 2 instrument from Bruker (Billerica, USA), equipped with a Cu anode and a Lynxeye detector.
The morphology of the formed calcium sulfate crystals was characterised by bright-field optical microscopy on an Eclipse E400 biological microscope from Nikon (Tokyo, Japan), equipped with objective lenses providing 5x, 10x, 25x and 50x magnification in addition to an inherent magnification of 10x. Images were taken with an EOS 50D digital camera from Canon (Tokyo, Japan), which was mounted on the microscope by an adapter from LMscope (Graz, Austria). Prior to imaging, the isolated powders were dispersed in anhydrous glycerol and positioned on a microscope slide. The hydration behaviour of the precipitated hemihydrate material was investigated by means of conductometry. For this purpose, 2 g solid product was added to 40 g water under vigorous stirring and the conductivity of the resulting suspension was monitored over time by an immersed conductometric sensor from Metrohm (5-ring conductivity measuring cell, c = 0.7 cm^{-1}, No. 6.0915.100) attached to an 856 Conductivity Module (No. 1.856.0010). The sensor was previously calibrated using KCl standard solution (Metrohm, No. 6.2301.060). As a reference, commercial bassanite obtained from flue gas desulfurisation at the power plant Schwarze Pumpe (Spremberg, Germany) was examined in the same way.

Supplementary Figures

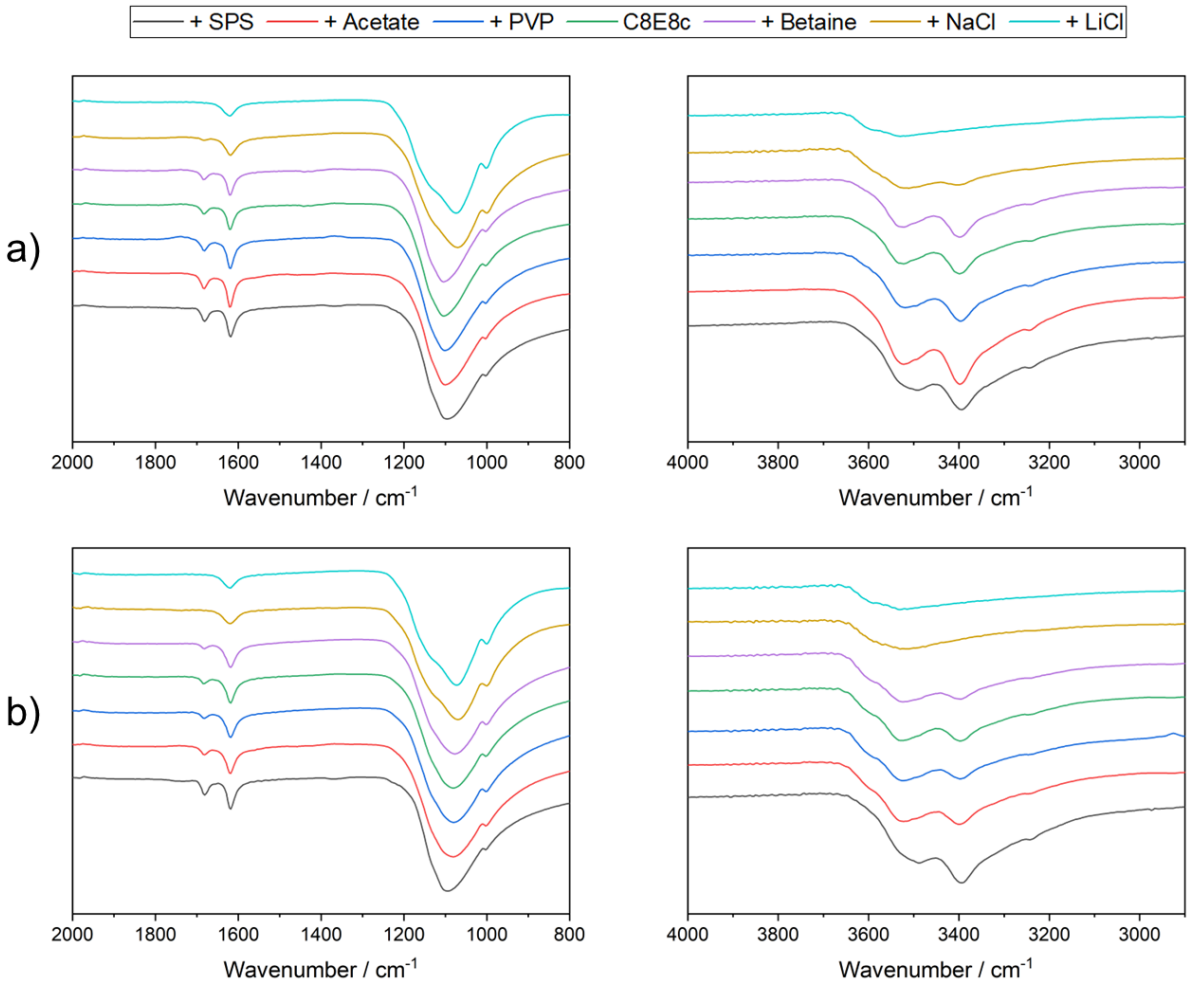

Figure S1. IR spectra of powders obtained from precipitation experiments at a) 25 °C and b) 40 °C as depicted by Figure 1 in the main text under conditions as specified in Table S1. Bassanite and gypsum can be distinguished by different spectral features originating from stretching vibrations of sulfate groups (left) and structural water (right). In particular, the band at 1684 cm^{-1} only occurs for gypsum and can be used to quantify the relative amounts of the two phases.[S1]

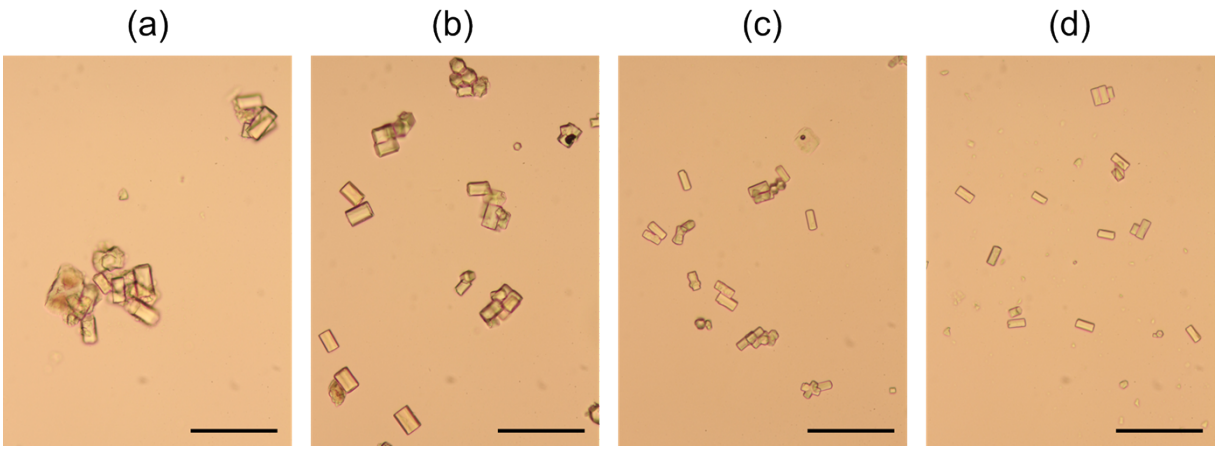

Figure S2. Optical micrographs showing typical bassanite particles obtained from precipitation experiments at 25 °C as depicted by Figure 1 in the main text from 0.4 M $CaSO_4$ solutions in the presence of a) 1 wt% C8E8c, b) 1 wt% C8E8c and 0.1 M betaine, c) 1 wt% C8E8c and 2.8 M NaCl, and d) 1 wt% C8E8c and 4.3 M LiCl. Under all conditions, blocky crystals with the characteristic equilibrium morphology of bassanite[S3] are observed. Typical particle sizes vary in the range of 20-30 µm in length and 10-20 µm in width, with on average smaller crystals being formed in the presence of excess electrolyte. Scale bars are 100 µm.

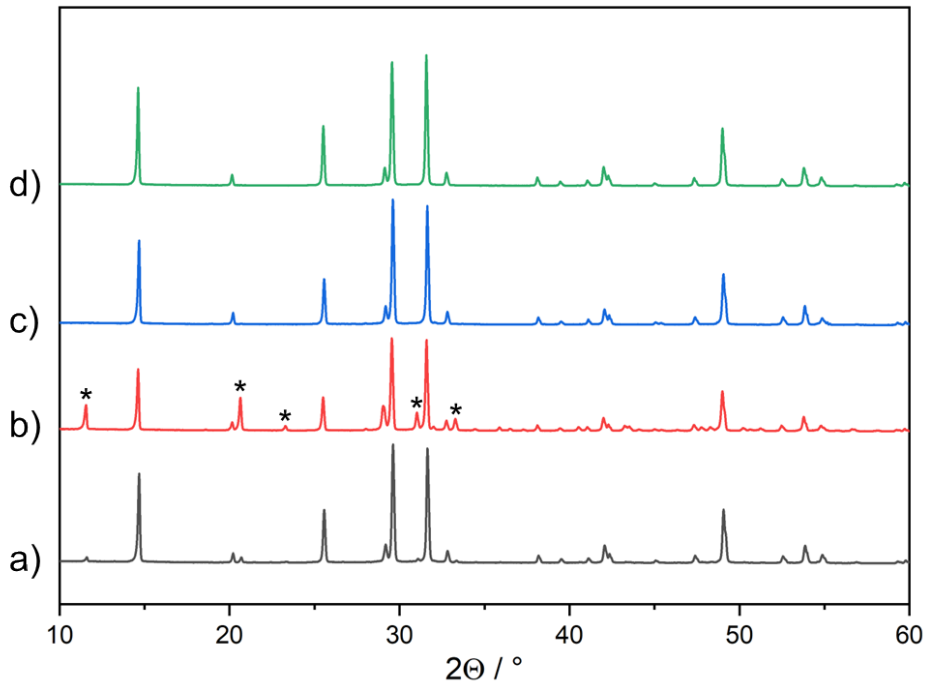

Figure S3. PXRD patterns of solid products recovered from $CaSO_4$ precipitation experiments in the presence of 1 wt% C8E8c and a) 4.3 M LiCl at 25 °C, b) 2.8 M NaCl at 25 °C, c) 4.3 M LiCl at 40 °C, and d) 4.3 M NaCl at 40 °C (i.e. the systems denoted as "1 wt% C8E8c + NaCl" and "1 wt% C8E8c + LiCl" in Figure 1 of the main text). All reflections observed for precipitates formed at 40 °C can be assigned to bassanite,[S4] while additional signals of gypsum (marked by asterisks) occur in the diffractograms of products obtained at 25 °C. The relative intensities of gypsum reflections agree well with the quantitative phase composition determined by IR spectroscopy (cf. Figure 1). Note the absence of any other crystalline phases such as NaCl, LiCl, Na_2SO_4 or Li_2SO_4.

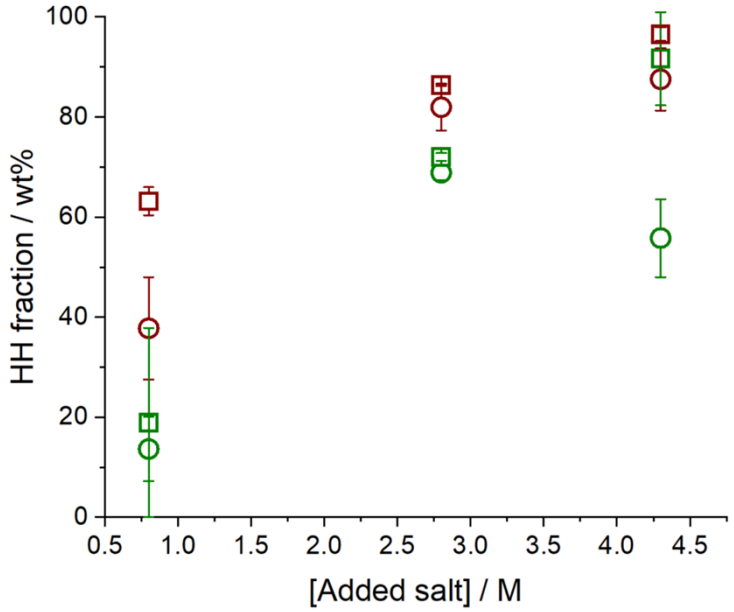

Figure S4. Plot of the weight fraction of bassanite in calcium sulfate precipitates formed at 25 (green symbols) or 40 °C (red symbols) as a function of the concentration of added NaCl (circles) or LiCl (squares). Symbols represent average values with their corresponding standard deviation obtained from at least two independent determinations.

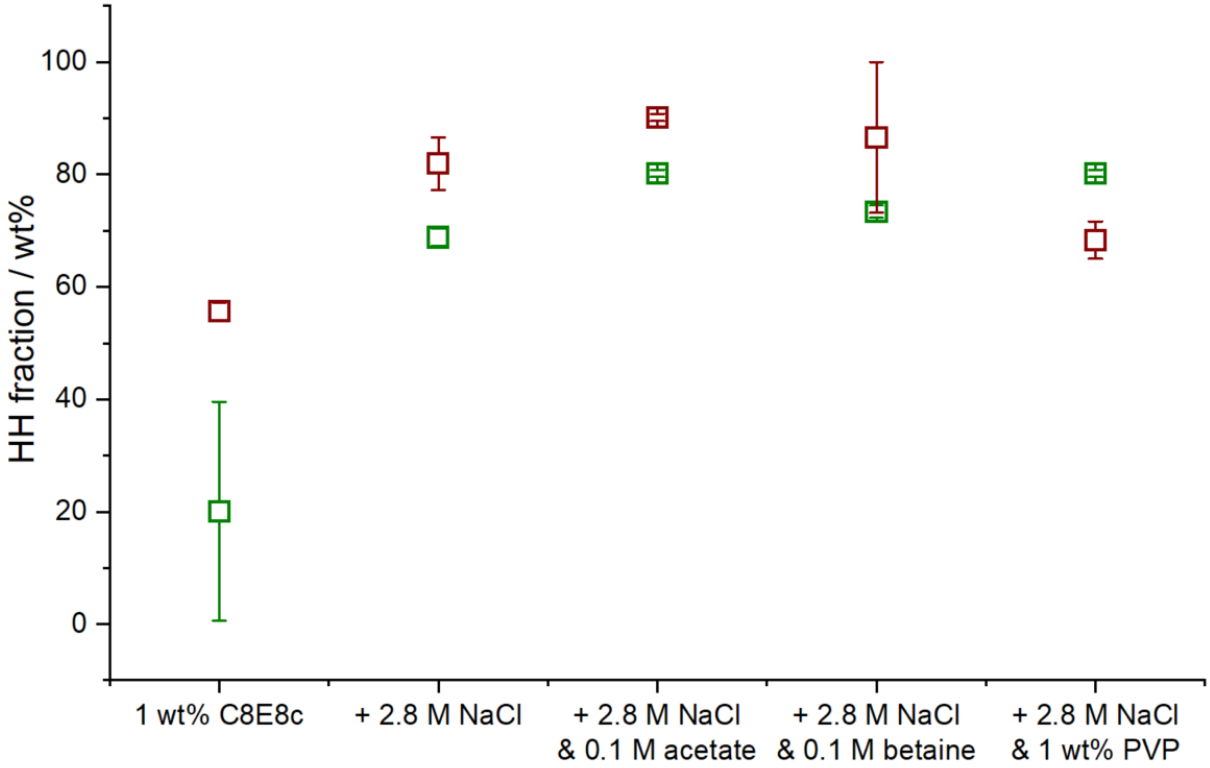

Figure S5. Plot of the weight fraction of bassanite in calcium sulfate precipitates formed at 25 (green symbols) or 40 °C (red symbols) from solutions of 1 wt% C8E8c, to which 2.8 M NaCl were given as secondary additive and 0.1 M acetate, 0.1 M betaine or 1 wt% PVP as third additive. Symbols represent average values with their corresponding standard deviation obtained from at least two independent determinations.

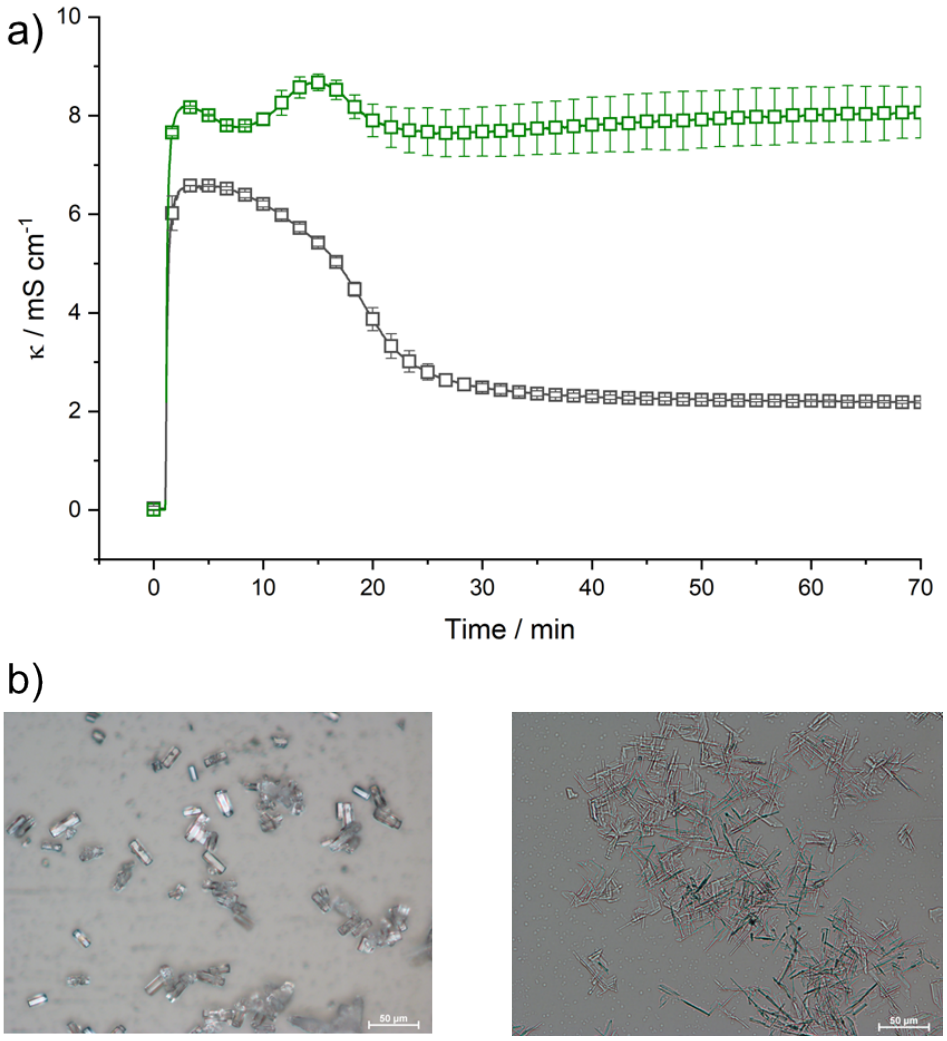

Figure S6. Characterisation of the hydration behaviour of bassanite powders in water at 23 °C. a) Time-dependent evolution of specific conductivity in 5 % (w/w) suspensions of conventional hemihydrate binder (black) and products obtained by precipitation from 0.4 M $CaSO_4$ solution in the presence of 1 wt% C8E8c and 4.3 M LiCl at 25 °C (green). Symbols represent average values with their corresponding standard deviation obtained from at least two independent determinations. With conventional bassanite, a steep increase in conductivity is observed upon addition of the solid powder to water (at ca. 1 min) up to 6-7 mS/cm, which corresponds to the solubility of the hemihydrate. Subsequently, conductivity decreases gradually with proceeding transformation to gypsum, which is essentially completed after about 30 min, where a constant level of κ ≈ 2.3 mS/cm is reached (solubility of gypsum). Overall, these observations are consistent with the results of previous studies on the hydration of bassanite to gypsum by conductometric monitoring.[S5] Hemihydrate materials prepared by precipitation in the present work show generally similar behaviour, yet with two significant differences: on the one hand, conductivity levels measured upon initial bassanite dissolution as well as after completed transformation to gypsum are higher than for conventional hemihydrate. This finding can be explained the presence of (soluble) sodium and lithium sulfate in the precipitated products (cf. Table S2). On the other hand, κ = f(t) profiles acquired for bassanite obtained via the method described in the present work show a minimum at ca. 8 min followed by a second maximum around 15 min before conversion to gypsum is completed. This might hint at differences in the transformation mechanisms, for example the temporary stabilisation of an intermediate phase such as amorphous calcium sulfate. In any case, hydration of precipitated bassanite to gypsum takes place within less than 30 min and is hence not slower than the corresponding reaction of conventional hemihydrate binders. b) Optical micrographs of bassanite particles obtained by precipitation from 0.4 M $CaSO_4$ solution in the presence of 1 wt% C8E8c and 4.3 M LiCl at 25 °C (left) and characteristic needle-shaped gypsum crystals formed upon hydration (right).

Supplementary Tables

Temperature	Additive	Concentration	Temperature	Additive	Concentration
25 °C	SPS	0.8 M	40 °C	SPS	0.8 M
	Acetate	0.2 M		Acetate	0.2 M
	PVP	1 wt%		PVP	1 wt%
	Betaine	0.1 M		Betaine	0.4 M
	NaCl	2.8 M		NaCl	4.3 M
	LiCl	4.3 M		LiCl	4.3 M

Table S1. Concentrations of the different additives, at which the respective highest fraction of bassanite could be recovered from precipitation experiments in the presence of 1 wt% C8E8c at 25 and 40 °C (data shown in Figure 1 of the main text).

	C8E8c + NaCl		**C8E8c + LiCl**	
	25 °C	40 °C	25 °C	40 °C
	Elemental fraction [wt%]			
C	n.d.	n.d.	n.d.	n.d.
H	1.40	0.90	1.10	1.00
O	51.97	47.10	51.01	51.11
Ca	21.40	19.60	22.20	22.30
S	20.40	11.88	21.30	21.40
Na	4.70	7.04	3.70	3.60
Li	n.d.	n.d.	0.41	0.42
Cl	0.13	1.50	0.28	0.09
	Calculated composition [mol%]			
$CaSO_4$	40.01	40.56	43.61	44.53
$(Na,Li)_2SO_4$	7.66	12.98	8.69	8.88
(Na,Li)Cl	0.27	6.78	0.62	0.38
H_2O	52.04	37.03	42.97	39.70

Table S2. Results of elemental analyses performed on solid products recovered from precipitation experiments at 0.4 M $CaSO_4$ in the presence of C8E8c and either sodium or lithium chloride at 25 and 40 °C (and additive concentrations as specified in Table S1). Levels of carbon were below the detection limit for all samples (n.d.: not detected), indicating the absence of significant amounts of organic species. Molar compositions were calculated under the assumption that all calcium ions exist in sulfate phases (i.e. not as calcium chloride).

References

[S1] Reigl, S.; Van Driessche, A. E. S.; Mehringer, J.; Koltzenburg, S.; Kunz, W.; Kellermeier, M. Revisiting the roles of salinity, temperature and water activity in phase selection during calcium sulfate precipitation. *Cryst. Eng. Comm.* **2022**, *24*, 1529-1536.

[S2] Reigl, S.; Van Driessche, A. E. S.; Wagner, E.; Mehringer, J.; Montes-Hernandez, G.; Koltzenburg, S.; Kunz, W.; Kellermeier, M. Toward more sustainable hydraulic binders: controlling calcium sulfate phase selection via specific additives. *ACS Sustainable Chem. Eng.* **2023**, *11*, 8450-8461.

[S3] Yeandel, S. R.; Freeman, C. L.; Harding, J. H. A general method for calculating solid/liquid interfacial free energies from atomistic simulations: application to $CaSO_4 \cdot xH_2O$. *J. Chem. Phys.* **2022**, *157*, 084117.

[S4] Tiemann, H.; Sötje, I.; Jarms, G.; Paulmann, C.; Epple, M.; Hasse, B. Calcium sulfate hemihydrate in statoliths of deep-sea medusae. *J. Chem. Soc., Dalton Trans.* **2002**, 1266-1268.

[S5] Wiegman-Ho, L.; Ketelaar, J. A. A. The kinetics of the hydration of calcium sulfate hemihydrate investigated by an electric conductance method. *J. Dent. Res.* **1982**, *61*, 36-40.